

The acoustic performance of the different types of plenum boxes for ceiling panels

Joanna Maria KOPANIA¹ , Grzegorz BOGUSŁAWSKI¹ , Kamil WÓJCIAK² , Patryk GAJ² 

¹ Lodz University of Technology, Żeromskiego 116, 90-924 Lodz, Poland

³ Institute of Power Engineering, Mory 8, 01-330 Warsaw, Poland

Corresponding author: Joanna Maria KOPANIA, email: joanna.kopania@p.lodz.pl

Abstract The aerodynamic noise generated by side entry plenum boxes intended for ceiling diffusers was studied. The plenum boxes in the inflow duct were tested in an anechoic room at low to moderate Reynolds numbers. Two characteristic phenomena were discussed: a way of fixing the cross-bar into the plenum box and vertical or horizontal throttle placement on the junction of the channel and plenum box on the acoustic parameters of plenum boxes. The characteristic peak in the L_{Aeq} spectrum moves to the higher frequencies with increased flow velocity linked with the flow around the crossbar inside the boxes. Additionally, the different positions of the throttle inside the plenum box were important for the acoustic parameters of the studied boxes. The vertical and horizontal positions of the throttle give various signals in the acoustic spectrum of studied objects.

Keywords: noise, ventilation, plenum box, cross-bar, throttle.

1. Introduction

Since most individuals spend 90% of their time indoors these days [1, 2], having a comfortable indoor environment is essential to daily living, employment, and education. It can be annoying to hear the noise from the daily activity of neighbourhoods [3, 4] but also from air conditioning or ventilation ducts in buildings [5-7]. The air distribution duct systems in the building contribute to the propagation of noise from the sources to the inhabitants. The fans, dampers, diffusers, and connectors inside the ducts may produce sound due to the airflow passing around them. Therefore, it is crucial to consider each additional element in the ductal system. Both upstream and downstream pathways are frequently equally significant because sound travels efficiently in the flow direction or in the opposite direction. Spectral features are the differences in frequency distributions of sounds produced by different sources [8].

The ventilation and air conditioning systems produce two categories of noise: propagated noise and self-noise. Rigidly fastened ventilation equipment to a slab, wall, or ceiling can create extremely undesired levels of structure-borne noise by transferring vibrations into the supporting structure. This noise has a long range and may even reverberate throughout the structure. Rigidly attaching ventilation system components to vibrating machinery, such as piping or ducts, has the potential to transfer noise into the structure. Additional causes of noise and vibration may include loose joints, general component wear, or tiredness. Self-noise refers to the turbulent noise present in specific local ductwork components. For instance, low frequencies dominate the spectrum of propeller fans, a phenomenon known as the blade-pass frequency. People sometimes compare the sound of a propeller fan from a duct to that of a helicopter [9]. Noise isolation techniques of the ventilation system (e.g., putting silencers in fans or ductwork) and combination mode adjustment can be used to minimise propagating noise. However, reducing noise in the ducts remains a significant issue, especially when considering the material or construction aspects of the ducts.

Ensuring adequate air distribution in the treated room is a crucial responsibility of the ventilation system, which is largely dependent on the geometry and placement of the supply air devices in the room. A ceiling diffuser is most likely the most commonly used air terminal device. The type of air diffuser and its supply air parameters are the primary factors that dictate the distribution of air in a room. The literature contains a variety of research investigations on the distribution of air from ceiling diffusers [10, 11], including measurement [12-14] and numerical calculation studies [15, 16].

Usually, a plenum box with a side (vertical) or top (horizontal) entry connects the diffusers to the installation. The type of plenum box used is one of the primary components that has a significant impact on the distribution of air velocity passing through the diffuser. Perforated panels sometimes equip plenum

boxes, ensuring proper and uniform distribution of the air stream and throttle in a short inlet duct. The airflow from the plenum box with side entry is highly asymmetrical [17], while velocity distribution from the diffuser is uniform for the top entry plenum box [18]. While a plenum box with a vertical duct connection guarantees superior conditions for symmetrical discharge at the diffuser. In practical applications, suspended ceiling space is limited, leading to a preference for plenum boxes with horizontal duct connections. Plenum boxes are often placed between the outlet of a fan and main air distribution ducts to smooth turbulent airflow. These boxes are lined with acoustically absorbent material to reduce noise. Based on earlier work, the acoustic parameters associated with a plenum box can be expressed using the following considerations: frequency range (above versus below the cut-off frequency), in-line inlet and outlet openings (no offset angle), and end-in/end-out versus end-in/side-out orientation [19-21]. Regarding the ceiling diffuser geometry, it is known that these objects usually have axial symmetry. However, the velocity fields under the diffusers show no axial symmetry. This asymmetry may produce uneven thermal conditions and increase air velocity in some parts of the room-occupied zone. When the air movement is too rapid, room occupants may experience discomfort due to the increased body heat losses from their skin, resulting in a greater cooling effect. This could potentially be the reason for the increased noise coming from the plenum box and the ceiling diffuser.

Understanding the behaviour of the airflow and its connection with the acoustics of a ventilated room is essential for designers to provide the most efficient ventilation system. Designers typically select air supply devices based on discharge data provided by equipment manufacturers. However, this approach, without the acoustical parameters, could potentially result in unsatisfactory solutions for the entire building's ventilation system. In this work, our research focuses on the aerodynamic noise generated by side entry plenum boxes, which are commonly used in ventilation systems and intended for ceiling diffusers. We examined the acoustical properties of the two types of plenum boxes with various throttle alignments in the inflow duct. We conducted the studies in an anechoic room at low to moderate Reynolds numbers using a specially constructed test stand. We determined the sound pressure level of boxes at various flow velocities using an acoustic camera and a sound pressure level analyser. This enabled the identification of the physical source of aerodynamic noise, a crucial consideration for such ventilation objects.

2. Experimental study

2.1. Studied models

In this study, we used commonly available galvanised steel plenum boxes, as shown in Fig. 1. We constructed the plenum boxes as an "empty" cube, measuring approximately 593 x 593 x 330 mm (height x width x depth), and incorporated a 40 mm wide cross-bar with a threaded hole in the centre to facilitate a swift and straightforward installation of the ceiling panel air diffuser. Box 1 has the cross-bar installed 40 mm below the outlet, but in the centre of the bar there is also the small L-shaped steel bar (38 mm long) with a hole for mounting the diffuser. Box 2 has the cross-bar installed 10 mm below the outlet, with a centre hole for mounting the diffuser. The plenum box was made from two sheets of steel with a thickness of 1 mm, riveted in the corners. It has a side entry connection that is appropriate for a 248 mm diameter duct. The throttle, made from a perforate plate, controls the flow volume of a short inlet duct (250 mm) leading to a plenum box. The inlet throttle operates from full closure to full opening to control the air volume. The plenum box's outlet incorporates a small steel edge, measuring 10 mm in width, to secure the air diffuser.

The aeroacoustic parameters of the plenum box were studied in two configurations of throttle at the duct inlet to the plenum box. A modification of the vertical and horizontal axes of rotation changed the throttle's position. The throttle in the plenum box possessed a horizontal axis of rotation, which could be locked up towards the outlet and bottom of the plenum box (either the ceiling diffuser panel or the box floor). Additionally, we changed the throttle's position to rotate along a vertical axis. In this position, the throttle was facing the right or left side of the plenum box, directing air flow from the duct. This study examined two throttle configurations in the plenum box and their impact on acoustical parameters:

- horizontal axis of rotation, fully opened, angle of position 0°;
- vertical axis of rotation, fully opened, angle of position 0°.

Two important things were considered in this study:

- Could the position of the crossbar inside the plenum box influence its acoustics?
- Is the throttle's vertical or horizontal localisation at the junction of the channel and plenum box possible to influence the sound pressure level?

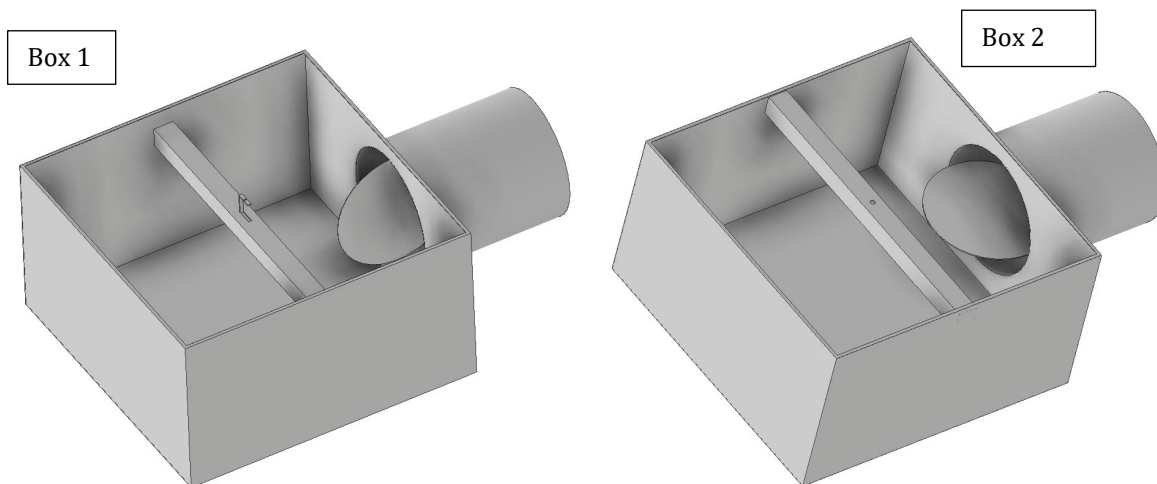


Figure 1. Scheme of studied plenum boxes: on the right - with horizontal axis of rotation (box 2 - on the right) and vertical axis of rotation the throttle (box 1 - on the left).

2.2. Aeroacoustic measurements

The measurements were performed on the special constructed test stand with the outlet to the anechoic room – Figure 2.

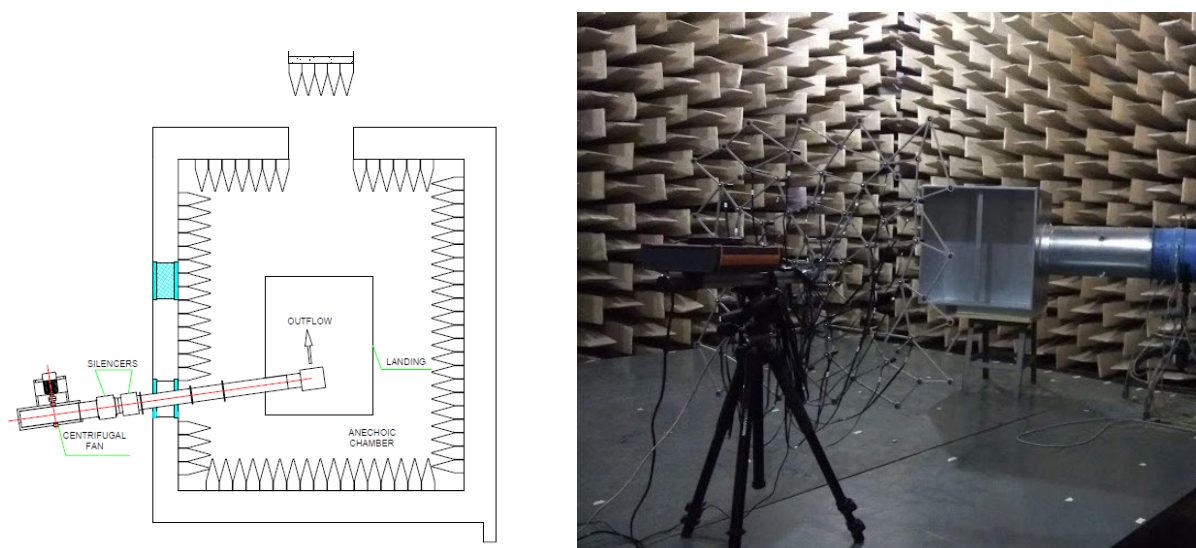


Figure 2. Scheme of test stand in the anechoic chamber.

Airflow was induced by a fan mounted on the inlet of the stand and regulated by the power inverter. The outlet of test stand was in the anechoic room at the Institute of Power Energy “ITC” in Lodz. The anechoic test chamber is cubic, approximately 350 m³ in size and has walls that are acoustically treated with foam wedges providing a reflection free environment. The measurements were taken at four flow velocities: 2 m/s; 5 m/s; 10 m/s and 15 m/s. Flow velocity was measured using the Prandtl tube according to norm PN-ISO 5221:1994 “Air distribution and air diffusion - Rules to methods of measuring air flow rate in an air handling duct”. To measure the far-field noise was made by:

- sound pressure level analyser. The microphone was located at a distance 1 m from front of the box and directed against to the direction of the flow. To provide isolation from wind noise, wind socks were placed on this microphone. The microphone was calibrated calibrator before commencing the acoustic test. In order to know how the changing of flow velocity influences the acoustics of the studied plenum boxes, the 2-D acoustic maps were made. The 2-D acoustic maps were done by using bicubic interpolation depending on the obtained parameters for the studied boxes. The bicubic interpolation can achieve good performance because it assumes the smoothness of the obtained data.

Bicubic interpolation processes 4x4 (16-pixel) squares and is often chosen because of this, but it takes more time to process;

- acoustic camera (Noise Inspector), with 40 MEMS microphones and HD camera and software which allow real-time sound imaging for quick results. The microphones were not calibrated before the measure because of due to the construction they not require frequent calibration.

Arrays of microphones (acoustic cameras) can be geometrically arranged, and the sound captured can be used to extract information about the geometrical location of a source. The goal of beamforming is to “steer” a “beam” towards the source of interest and to pick its contents up in preference to any other competing sources of noise. This study employed the Delay & Sum Technique [22], which is the oldest, highly competitive, and simple method. The images from the acoustic camera were taken at the same distance as the analyser measurements.

3. Discussion of the results

3.1. Measurements by sound pressure level analyser

Figure 3 displays the A-weighted equivalent continuous sound level at box 1’s outlet based on the studied velocities. We observed the following peaks independent on the flow velocities:

- at 160 Hz, the signal may represent a measurement environment, specifically a hard platform where the stand test is located;
- at 500 Hz, especially at 2 m/s and 5 m/s - what could be connected with the flow fan sound;
- and also at 1000 Hz, probably coming from expansion the duct flow to plenum box.

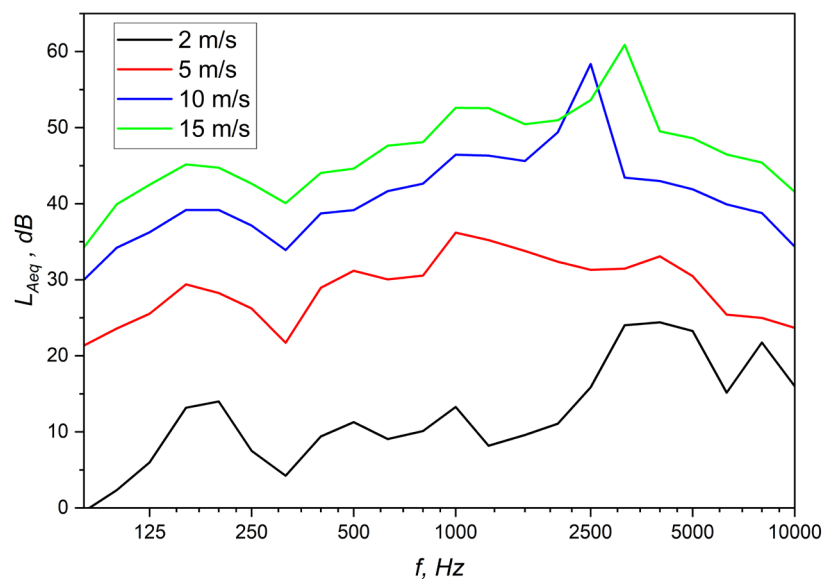


Figure 3. The octave of box 1's A-weighted equivalent continuous sound level depends on the airflow velocities.

Two peaks at 3150 Hz and 5000 Hz in the spectrum of box 1 at 2 m/s were observed. They turn into one peak at 4000 Hz at 5 m/s, followed by another peak at 5000 Hz at 15 m/s. This phenomenon may be caused by a tiny element in the plenum box, such as the cross-bar, vibrating and producing the aeolian tone in this range of frequencies. There is also something interesting at the higher velocities. The one strong peak at 2500 Hz at 10 m/s and 3150 Hz at 15 m/s is observed. It is difficult to explain the observed peaks, but if the peaks move towards the higher frequency at higher airflow velocities, that may be connected also with the produced sound into the plenum box. Figure 4 displays the A-weighted equivalent continuous sound level at box 2’s outlet based on the studied velocities. Also, the peak at 160 Hz, 500 Hz (well seen at 2 m/s), and 1000 Hz are observed independent of the flow velocities. At the lowest velocity of 2 m/s, the peaks at 1600 Hz and around 5000 Hz are observed. Peak at 1600 Hz is also observed at 10 m/s, but at 15 m/s it is moving to the 2000 Hz. Peak at 5000 Hz is observed only at 5 m/s because at higher velocities it disappears in noise or gets distracted.

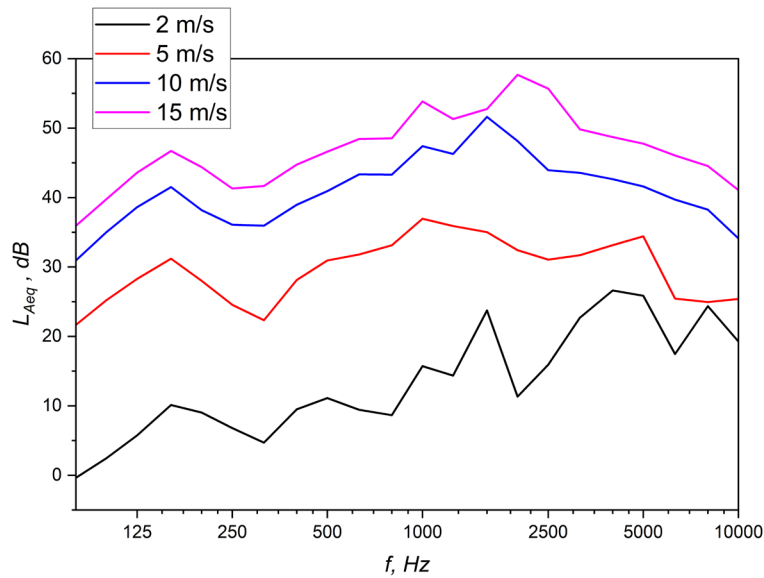


Figure 4. The octave of box 2's A-weighted equivalent continuous sound level depends on the airflow velocities.

Figures 5 and 6 present the normalized acoustic 2-D maps for the studied boxes, ranging from 2 m/s to 15 m/s. These maps show no significant differences up to 3000 Hz. We observe an increase in L_{Aeq} values between 1000 and 1600 Hz in both cases. For plenum box 1, the region of interest is at higher frequencies, where we observe an increase as the velocity increases. We observe the yellow-orange area above 5000 Hz at 15 m/s. The red area (the highest frequency peak) on this map is around 7000 Hz between 9 and 15 m/s. Box 2 has three acoustic-sensitive areas: the aforementioned range of 1000–1600 Hz, above 5000 Hz, and between 6000 and 7000 Hz. These maps reveal the importance of the higher range of frequencies in the spectrum of the studied boxes. It can be assumed that boxes behave as a room containing a diffuse sound field composed of many component waves reflected from the walls and also a direct sound field representing the effects of any sound waves entering the room and transmitted to the observation point without reflection. Cummings presented this problem [23], modelling such boxes based on Weel's theory [19]. However, based on these studies, determining which frequencies correspond to the box's housing, throttle, or cross-bar remains a challenge.

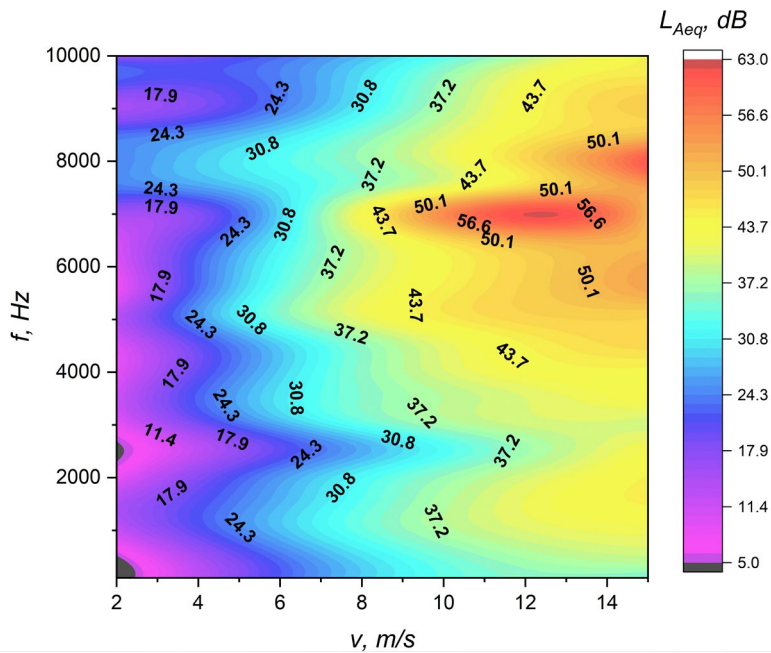


Figure 5. The acoustic map of changing the A-weighted equivalent continuous sound level depends on the flow velocities for box 1.

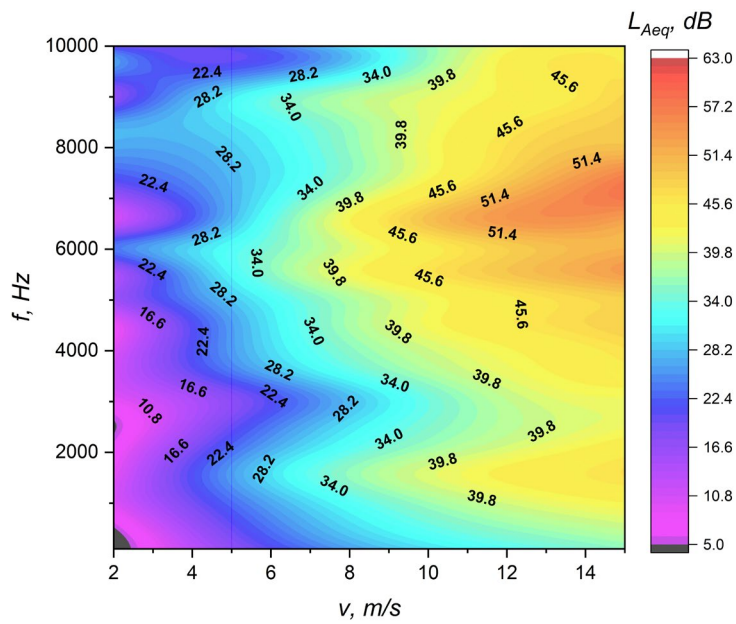


Figure 6. The acoustic map of changing the A-weighted equivalent continuous sound level depends on the flow velocities for box 2.

3.2. Measurements by acoustic camera

The acoustic camera measurements reveal independent peaks at 160 Hz, 500 Hz, and 1000 Hz (Figure 7), which align with the analyser’s measurements. The peaks at 500 Hz and 1000 Hz come from airflow in the duct. We also observe a peak between 3000-5000 Hz (Figure 8), which is dependent on the flow velocity. The interaction between the airflow, throttle, and cross-bar in the centre of the plenum box connects to this peak. We have identified a single, robust peak at 2500 Hz at 10 m/s and a slightly weaker one at 3150 Hz at 15 m/s. The interaction between the throttle and the wall of the plenum box could explain this phenomenon. The airflow stream from the duct to the square plenum box, which limited the throttle located partially in the duct and in the box, could generate the acoustic signals (Figure 9). The low Mach number flow over such space is accompanied by a characteristic effect of the generation of sound with high intensity in narrow frequency bands. The frequency of the excited oscillation in the throttle and wall’s box changes as the flow velocity varies, and the range of this change depends on flow conditions (a laminar or turbulent boundary layer) and the reacting geometries of the object.

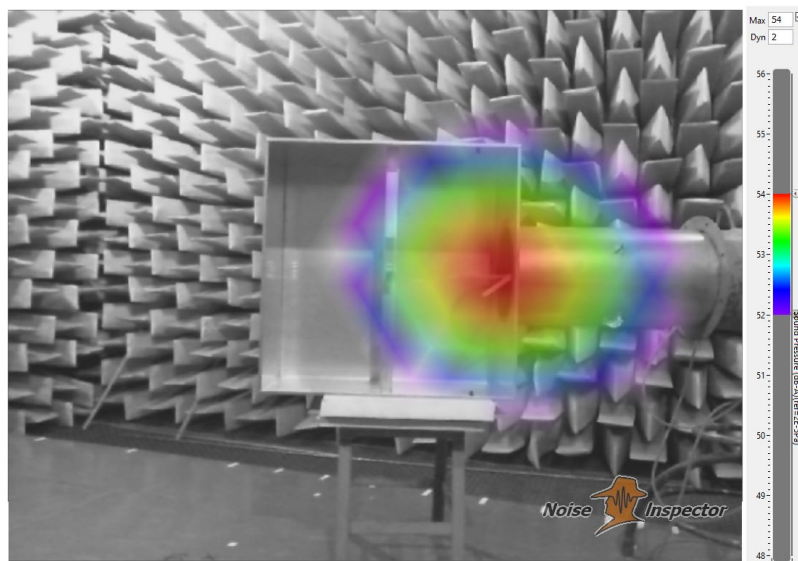


Figure 7. Calculated image by Delay and Sum algorithm from acoustic camera for box 1 at 1000 Hz at 10 m/s.

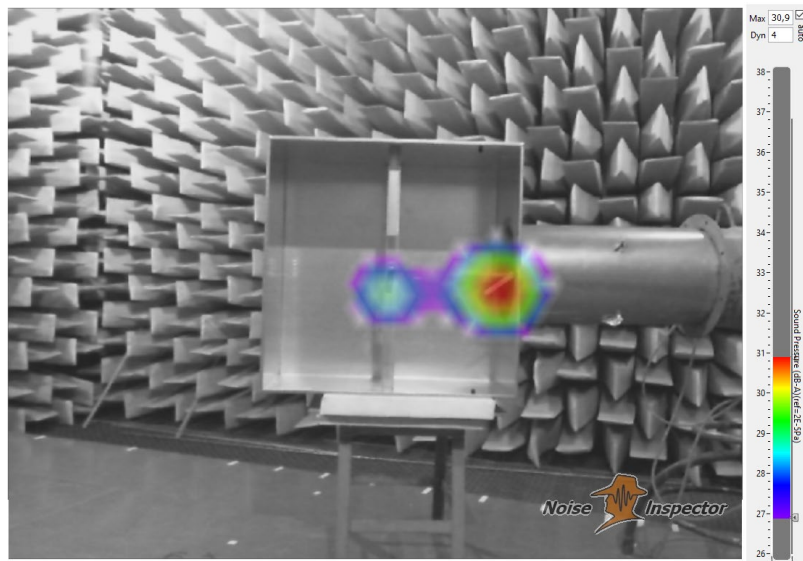


Figure 8. Calculated image by Delay and Sum algorithm from acoustic camera for box 1 at 4000 Hz at 5 m/s.

Figure 9 displays a discrete frequency that begins at 2500 Hz at 10 m/s and gradually increases to 3150 Hz at 15 m/s. This discrete sound can be generated by a flow over a space created by the throttle and side of the plenum box and is the effect of an interaction between disturbances of the shear layer and acoustic disturbances induced in a such space. There are several possible variants of flow-acoustic interactions that contribute to this effect. In this case, we have an open cavity. Open cavities are divided into two categories: shallow and deep, and the condition $l/d = 1$ sets the boundary between them, where l is the dimension of the opening of the cavity in the direction of flow and d is the depth of the cavity. In the case of a deep cavity, for which $l/d < 1$, the effect of discrete sound induction is related to the shear layer instability due to two factors. The influence of resonance modes of the cavity on disturbances of the shear layer is the first factor, while the second one is the flow-acoustic interaction at the leading and trailing edges. If only the first factor occurs in the process of sound generation, then the instability of the shear layer can take place solely for frequencies close to definite values, which are determined by the resonance condition for a quarter-wave resonator.

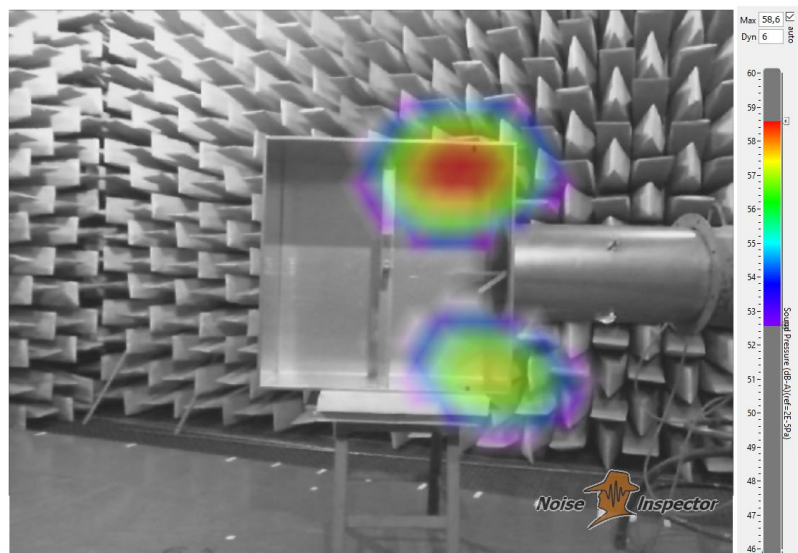


Figure 9. Calculated image by Delay and Sum algorithm from acoustic camera for box 1 at 2500 Hz at 10 m/s.

For box 2, similarly to the measurements obtained from analyser, the following peaks independent on the flow velocities are observed: at 160 Hz (linked to the environmental during the measurements), 500 Hz (derived from air flow from duct) and also at 1000 Hz and 1600 Hz.

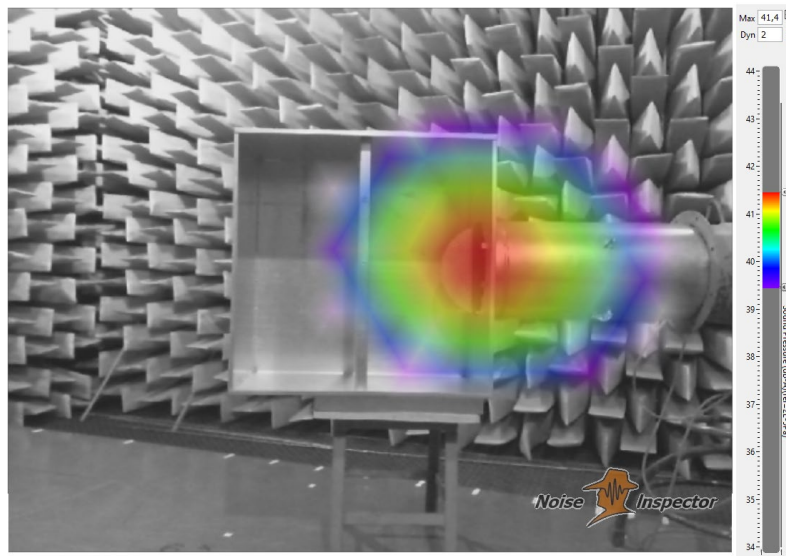


Figure 10. Calculated image by Delay and Sum algorithm from acoustic camera for box 2 at 1000 Hz at 5 m/s.

The peaks probably are connected with the flow around the throttle. The region of re-circulating flow, formed downstream of the throttle shaft (fixing of throttle), is known as the aerodynamic wake region - Figure 10 and Figure 11. The viscous air flow around the throttle plate surface causes air recirculation. The medium is displaced when it leaves the surface of throttle shaft, resulting in turbulent eddies being formed. The presence of eddies make the flow through the wake region turbulent what can influence on the acoustic signal from plenum box. The peak around 5000Hz is also observed. This peak is connected with the interaction between throttle and cross bar in the centre of plenum box, what we can see in Figure 12.

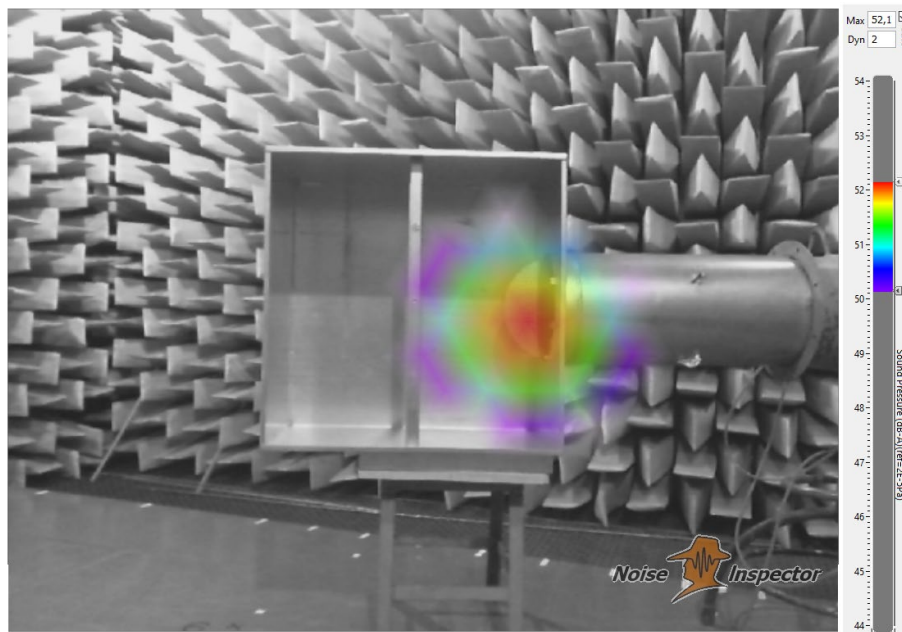


Figure 11. Calculated image by Delay and Sum algorithm from acoustic camera for box 2 at 1600 Hz at 15 m/s.

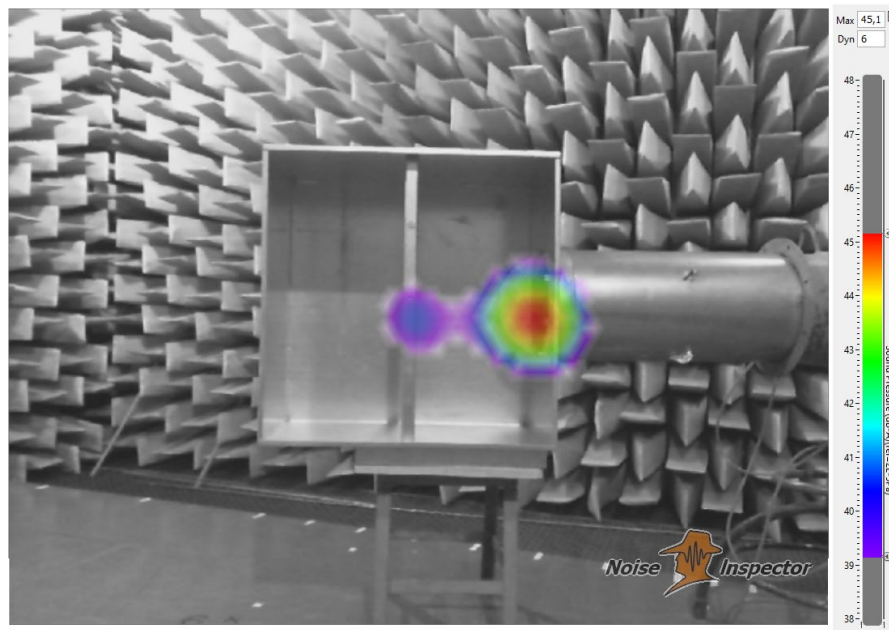


Figure 12. Calculated image by Delay and Sum algorithm from acoustic camera for box 2 at 5000 Hz at 15 m/s.

In the next stage, the A-weighted equivalent continuous sound level calculations were made. These values are important for architects and building designers. The L_{Aeq} values for each ventilation element in the whole system determine the noise in the whole installation, for example, according to ASHRAE's guide [24]. The single number L_{Aeq} for studied boxes is presented in Table 1. This table shows that at 2 m/s and 5 m/s, the lower values of L_{Aeq} correspond to box 1. However, at higher velocities, box 2 exhibits superior acoustics. Therefore, we cannot definitively state which box is superior as it relies on the flow velocity.

Table 1. A-weighted equivalent continuous sound level depends on the flow velocities obtained from analyser and acoustic camera for box1 and box 2.

v m/s	L_{Aeq} , dB			
	box 1		box 2	
	analyser	camera	analyser	camera
2	30.6	32.1	32.7	30.2
5	44.0	44.0	44.9	46.1
10	60.2	59.6	57.1	57.7
15	64.1	61.3	63.4	63.7

4. Conclusions

In this work, the aerodynamic noise generated by side entry plenum boxes intended for ceiling diffusers was studied. The two types of plenum boxes with various throttle alignments in the inflow duct were tested. The measurements were made in an anechoic room at low to moderate Reynolds numbers using a specially constructed test stand. The 1/3 octave A-weighted equivalent continuous sound levels depend on the flow velocities at various flow velocities, which were measured using an acoustic camera and sound pressure level analyser.

Two characteristic phenomena were discussed taking into account the acoustical parameters of the studied boxes: the cross-bar inside the boxes and the throttle localisation on the junction of the channel and plenum box. For box 1, two peaks at 3150 Hz and 5000 Hz at 2 m/s in the L_{Aeq} spectrum were observed. They turn into one peak at 4000 Hz at 5 m/s, followed by another peak at 5000 Hz at 15 m/s. For box 2, the peak around 5000 Hz is observed in both the analyser and acoustic camera studies. When an air stream passes across a rod with a different shape (e.g., cylindrical or square), vortices (eddies) are formed on the leeward side (backside). These vortices alternate from the top and bottom surfaces and create alternating pressures that tend to produce movement at right angles to the direction of the air flow. This is the

mechanism that causes aeolian vibration. So, the cross-bar in the centre of the plenum box may be the source of such vibration. In this work, the characteristic frequency at 5000 Hz becoming from cross-bar for studied plenum boxes was observed. As it turned out, the differences in construction of the cross-bar have not had an impact on the acoustic signals from the studied boxes.

The second issue is the position of the throttle inside the plenum box. It is important for the acoustic parameters of the studied boxes. In the vertical position of the throttle (box 1), two single, robust peaks at 2500 Hz at 10 m/s and a slightly weaker one at 3150 Hz at 15 m/s may be connected with the interaction between the throttle and the wall's box. For box 2, two peaks at 1000 Hz and 1600 Hz were observed, probably connected with the flow around the throttle. The region of re-circulating flow, formed downstream of the throttle shaft (fixing of throttle), is known as the aerodynamic wake region. The presence of eddies makes the flow through the wake region turbulent, which can influence the acoustic signal from the plenum box. This causes the higher L_{Aeq} values for box 2 at 2 m/s and 5 m/s (analyser measures). A precise description of the ceiling diffuser with plenum box and its acoustical parameters is necessary to forecast the air movement over the entire space. The behaviour of the airflow in the ventilated room must be understood by designers in order to develop the most efficient ventilation system with the lowest indoor noise.

Additional information

The authors declare: no competing financial interests and that all material taken from other sources (including their own published works) is clearly cited and that appropriate permits are obtained.

References

1. R. Ruparathna, K. Hewage, R. Sadiq; Improving the energy efficiency of the existing building stock: a critical review of commercial and institutional buildings; *Renew. Sustain. Energy Rev.*, 2016, 53, 1032–1045; DOI: 10.1016/j.rser.2015.09.084
2. M.C. White; Environmental protection agency; *Eos Transactions American Geophysical Union*, 1994, 75(7), 75; DOI:10.1029/94E000781
3. C. Díaz, A. Pedrero; Antonio; Sound exposure during daily activities; *Applied Acoustics*, 2006, 67, 271–283; DOI:10.1016/j.apacoust.2005.06.005
4. Jiannan Cai, Mei-Po Kwan, Zihan Kan, Jianwei Huang; Perceiving noise in daily life: How real-time sound characteristics affect personal momentary noise annoyance in various activity microenvironments and times of day; *Health & Place*, 2023, 83, 103053; DOI:10.1016/j.healthplace.2023.103053
5. M. Ghasemian, A. Nejat; Aerodynamic noise prediction of a horizontal Axis wind turbine using improved delayed detached eddy simulation and acoustic analogy; *Energy Convers. Manag.*, 2015, 99, 210–220; DOI: 10.1016/j.enconman.2015.04.011
6. O. Jianu, M.A. Rosen, G. Naterer; Noise pollution prevention in wind turbines: status and recent advances, *Sustainability*, 2012, 4(6), 1104–1117; DOI:10.3390/su4061104
7. S.K. Tang; Performance of noise indices in air-conditioned landscaped office buildings; *J. Acoust. Soc. Am.*, 1997, 102(3), 1657–1663; DOI:10.1121/1.420077
8. M. J. Crocker, *Handbook of noise and vibration control*, John Wiley & Sons, Inc., Hoboken, New Jersey, Chapter 10, pp. 1327–1330, 2007
9. N.P. Cheremisinoff; *Noise control in industry - a practical guide*, Noyes, USA, 1996
10. A. Li, C. Yang, T. Ren, X. Bao, E. Qin, R. Gao; PIV experiment and evaluation of air flow performance of swirl diffuser mounted on the floor; *Energy Build*, 2017, 156, 58–69
11. M. Hurnik, J. Kaczmarczyk, Z. Popiolek; Study of Radial Wall Jets from Ceiling Diffusers at Variable Air Volume; *Energies*, 2021, 14, 240
12. S. Shakerin, P. Miller; Experimental study of Vortex Diffusers; *ASHRAE Trans.*, 1996, 102, 340–346
13. M. Jaszczur, P. Madejski, M. Borowski, M. Karch; Experimental analysis of the air stream generated by square ceiling diffusers to reduce energy consumption and improve thermal comfort; *Heat Transfer. Eng.*, 2021, 43(3–5), 463–473, DOI: 10.1080/01457632.2021.1875169
14. M. Borowski, M. Karch, R. Łuczak, P. Zyczkowski, M. Jaszczur; Numerical and experimental analysis of the velocity field of air flowing through swirl diffusers; *E3S Web Conf.*, 2019, 128, 05003
15. M. Jaszczur, P. Madejski, S. Kleszcz, M. Zych, P. Palej; Numerical and experimental analysis of the air stream generated by square ceiling diffusers; *E3S Web Conf.*, 2019, 128, 08003
16. A. Nocente, T. Arslan, S. Grynning, F. Goia; CFD Study of Diffuse Ceiling Ventilation through Perforated Ceiling Panels; *Energies*, 2020, 13, 1995

17. R. Hongze, Z. Bin, L. Xianting, F. Hongming, Y. Xudong; Influence of Diffuser Jet Characteristics on Indoor Air Distribution under Actual Connecting conditions; *J. Archit. Eng.*, 2003, 9, 141–144
18. J.M. Villafruela, J.B. Sierra-Pallares, F. Castro, A. Álvaro, P. Santiago-Casado; Experimental and numerical study of the influence of the plenum box on the airflow pattern generated by a swirl air diffuser; *Exp. Therm. Fluid Sci.*, 2018, 99, 547–557
19. R.J. Wells; Acoustical plenum chambers; *Noise Control*, 1958, 4(4), 9–15; DOI: 10.1121/1.2369329
20. A. Cummings, A.M. Wing-King; The attenuation of lined plenum chambers in ducts, II: measurements and comparison with theory; *J. Sound Vib.*, 1979, 63(1), 19–32; DOI: 10.1016/0022-460X(79)90374-2
21. H.J. Kim, J.G. Ih; Rayleigh–Ritz approach for predicting the acoustic performance of lined rectangular plenum chambers; *J. Acoust. Soc. Am.*, 2006, 120(4), 1859–1870; DOI: 10.1121/1.2336748
22. D.H. Johnson, D.E. Dudgeon; *Array Signal Processing: Concepts and Techniques*, Prentice Hall Signal Processing Series, 1993
23. A. Cummings; The attenuation of lined plenum chambers in ducts, I: Theoretical models; *J. Sound Vib.*, 1978, 61(3), 347–373
24. M. A. Schaffer; *A practical guide to noise and vibration control for HVAC systems*, Second Edition, American Society of Heating, Refrigerating and Air-Conditioning Engineers, Inc., 2005

© 2025 by the Authors. Licensee Poznan University of Technology (Poznan, Poland). This article is an open access article distributed under the terms and conditions of the Creative Commons Attribution (CC BY) license (<http://creativecommons.org/licenses/by/4.0/>).